Electronic Supplementary Material (ESI) for Physical Chemistry Chemical Physics.

Supplementary Data

Molecular Mechanism of Ligand Unbinding from Human Telomeric G-quadruplex by Steered Molecular Dynamics and Umbrella Sampling Simulations

Jia-Kai Zhou[a], Dah-Yen Yang[b,†,*] and Sheh-Yi Sheu[a,c,†,*]

[a]Department of Life Sciences and Institute of Genome Sciences, National Yang-Ming University, Taipei 112, Taiwan
[b]Institute of Atomic and Molecular Sciences, Academia Sinica, Taipei 106, Taiwan
[c]Institute of Biomedical Informatics, National Yang-Ming University, Taipei 112, Taiwan

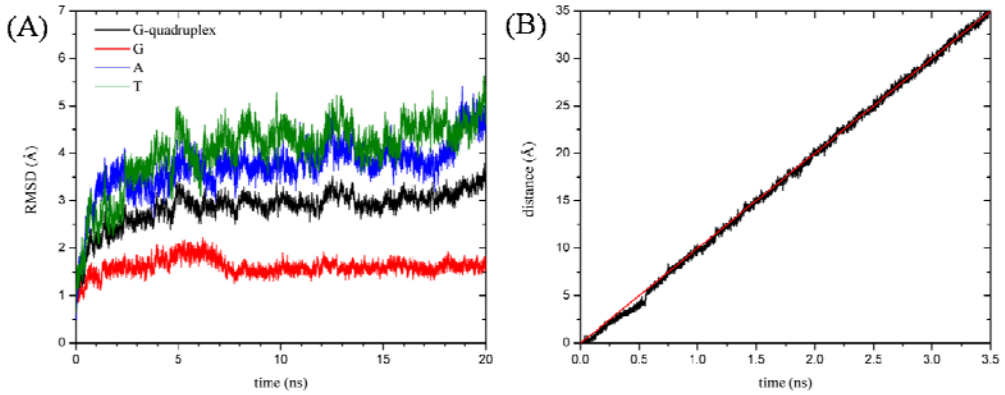

Figure S1: (A) RMSD plot of the G-quadruplex/BMVC complex structure during the MD simulation. The overall structure (black line), the G-quartet part (red line) and the loop part (the bases A and T) (blue and green lines) are shown. (B) Plot of the pulling distance (black line) and the constrained distance (red line) measured in the SMD simulation of the G-quadruplex/BMVC complex performed with the force constant 7.2 kcal/(mol Å^2) and the velocity 0.01 Å/ps along the reaction coordinate.

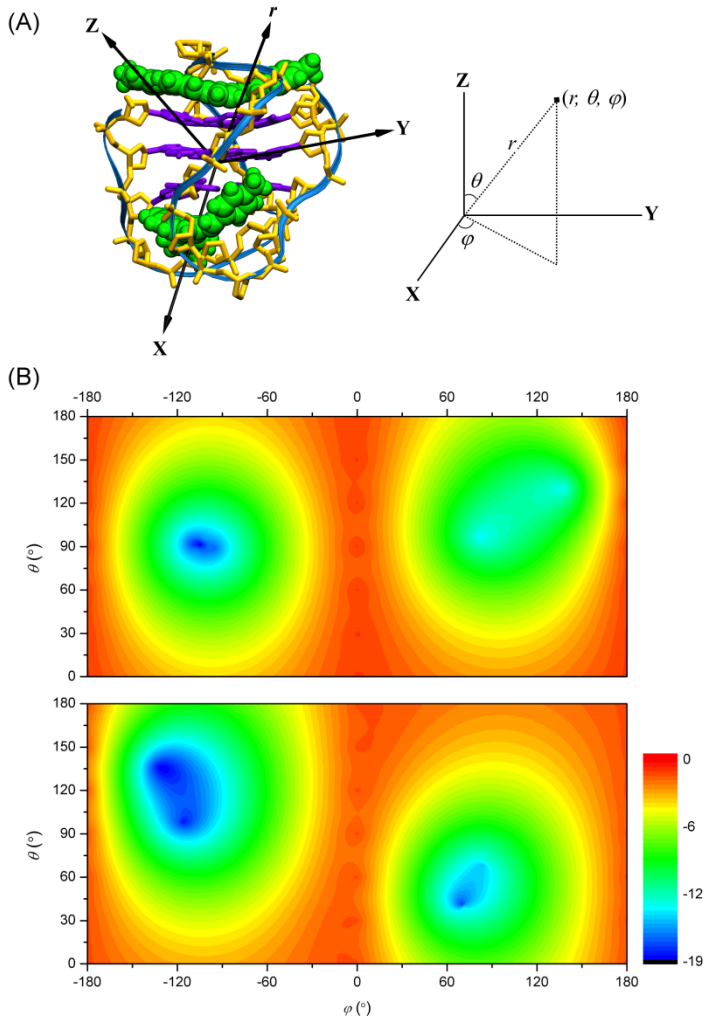

Figure S2: (A) Definition of the spherical coordinate in the G-quadruplex-BMVC complex. The X, Z and Y refer to the longest, second and third principal axes of the G-quadruplex, respectively. The $\vec{r}$ vector indicates the pulling direction. (B) Free energy contour map versus the angles (θ, φ) of BMVC unbinding from the diagonal loop (top panel) and parallel loop (bottom panel) of the G-quadruplex complex. Free energy unit is in kcal/mol.

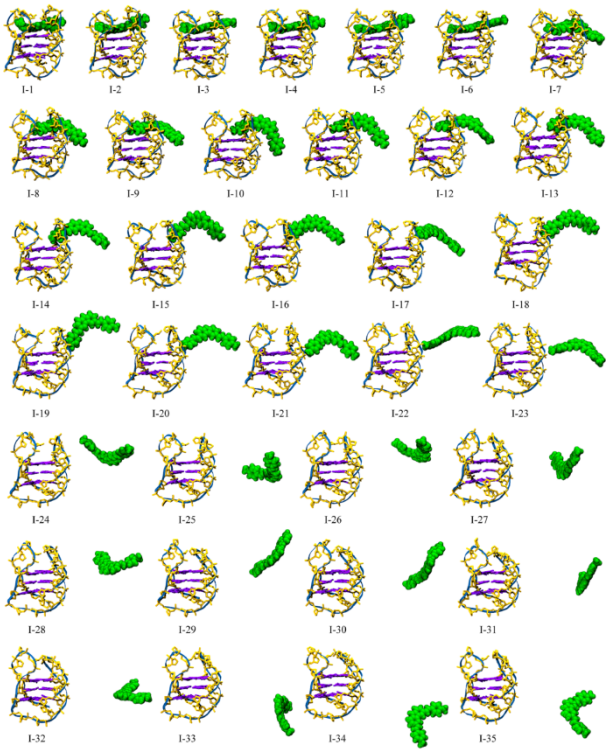

Figure S3-I: The snapshots of the unbinding pathway I. BMVC was directly drawn out from the G-quadruplex.

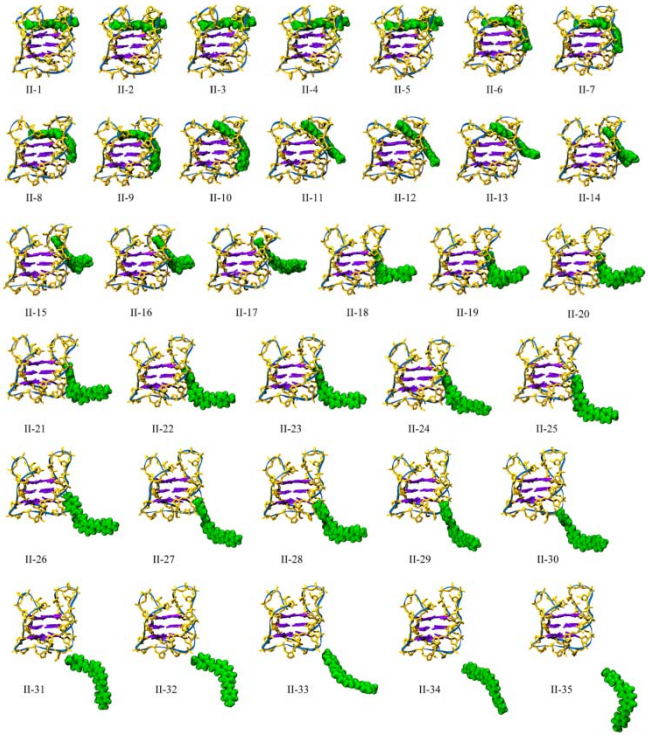

Figure S3-II: The snapshots of the unbinding pathway II. BMVC slides along the groove.

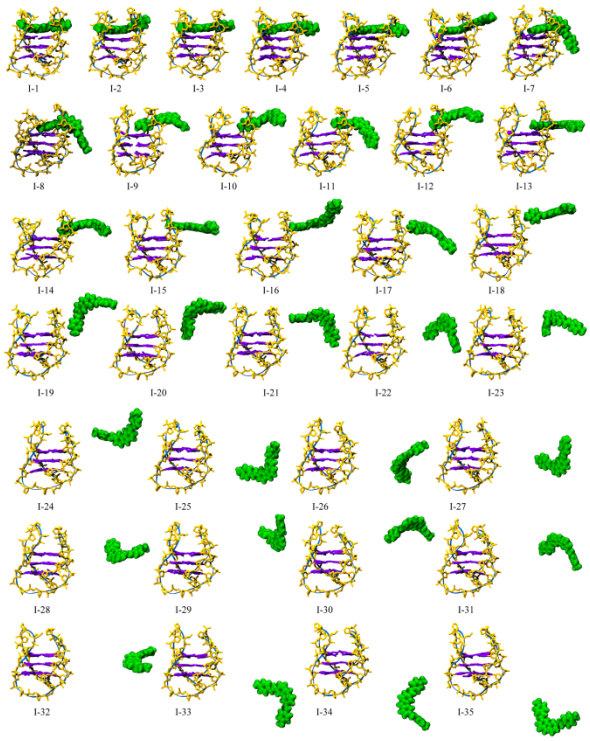

Figure S3-III: The snapshots of the unbinding pathway III. BMVC0 was directly drawn out from the G-quadruplex.

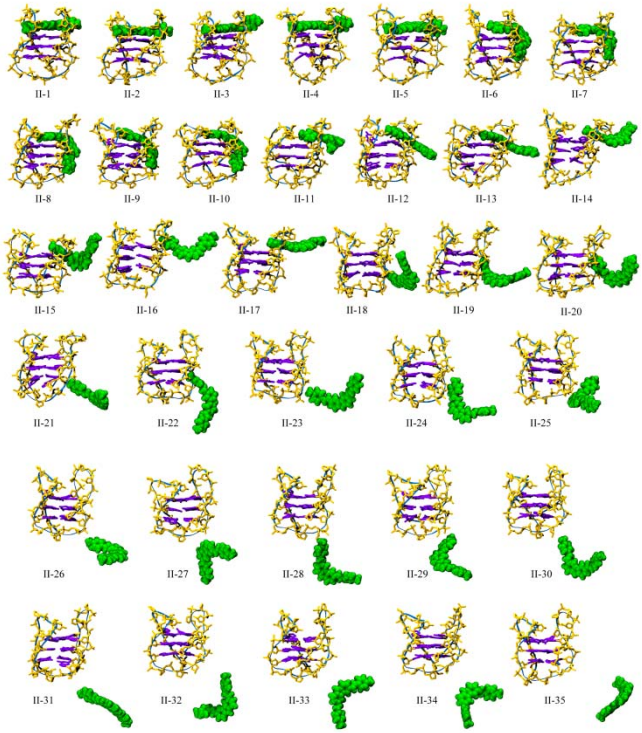

Figure S3-IV: The snapshots of the unbinding pathway IV. BMVC0 slides along the groove.

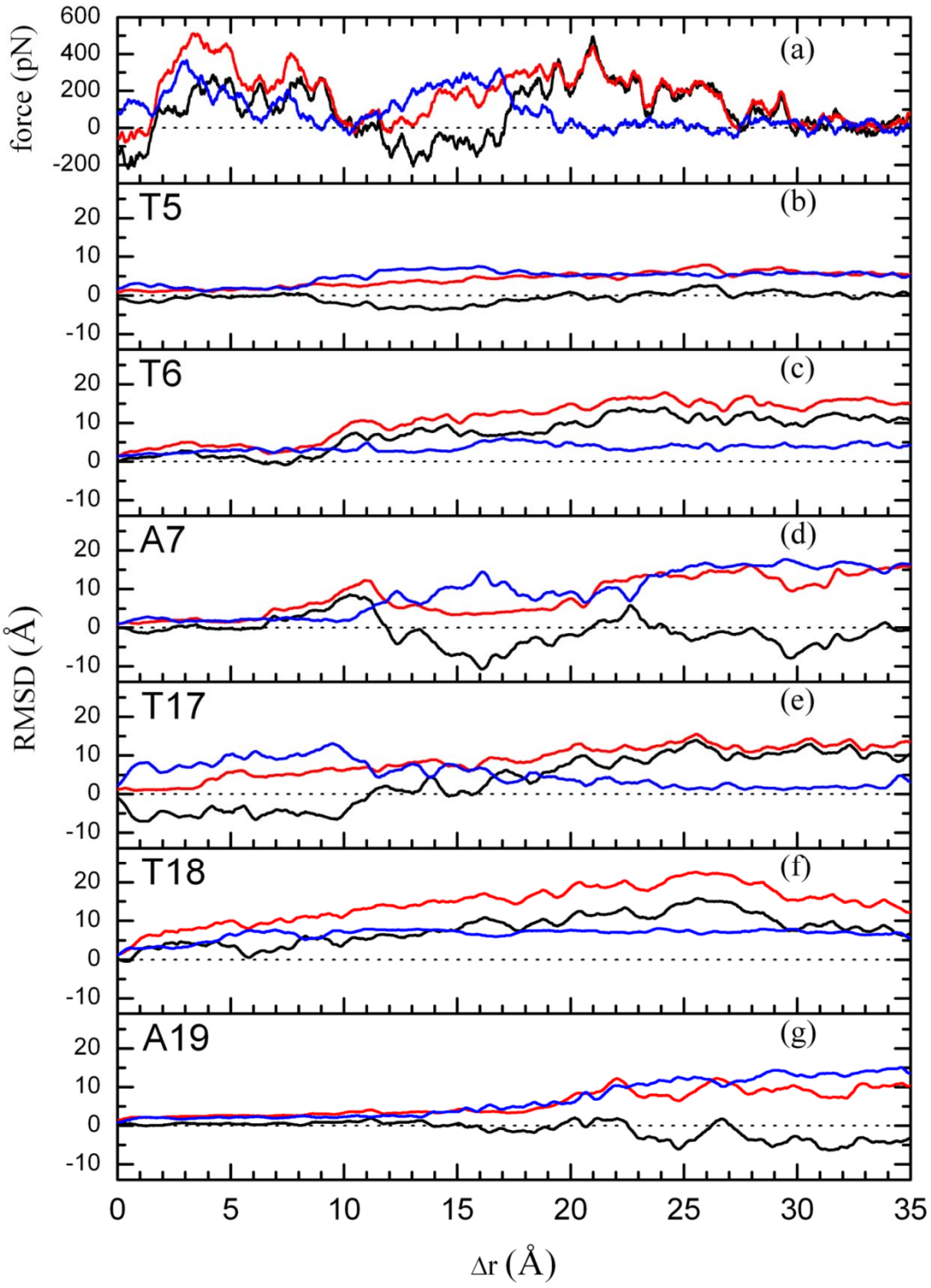

Figure S4: (a) The effective force as a function of the reaction coordinate and (b)-(g) RMSD as a function of the reaction coordinate. Black: the RMSD difference between BMVC and BMVC0. Red: BMVC. Blue: BMVC0.

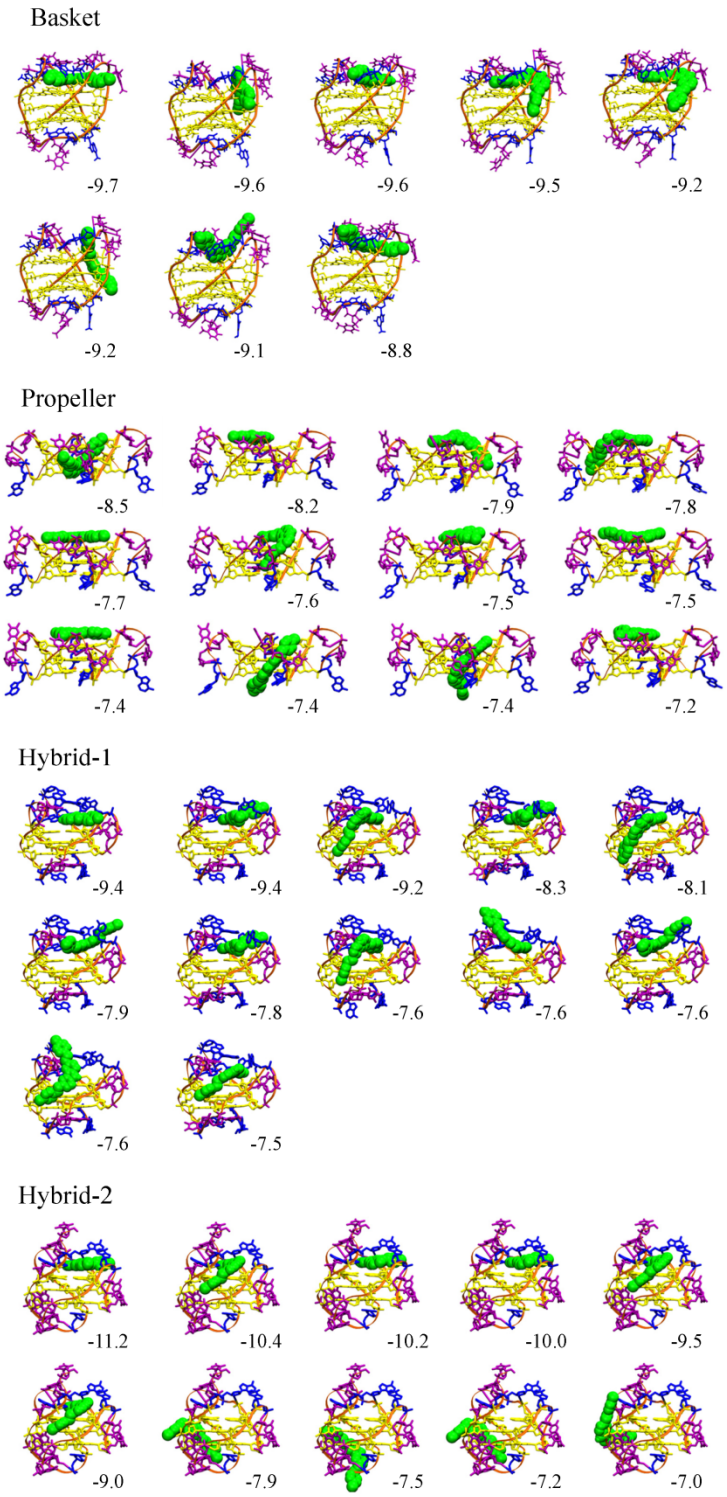

Figure S5: Docking complex structure and binding affinity (kcal/mol)

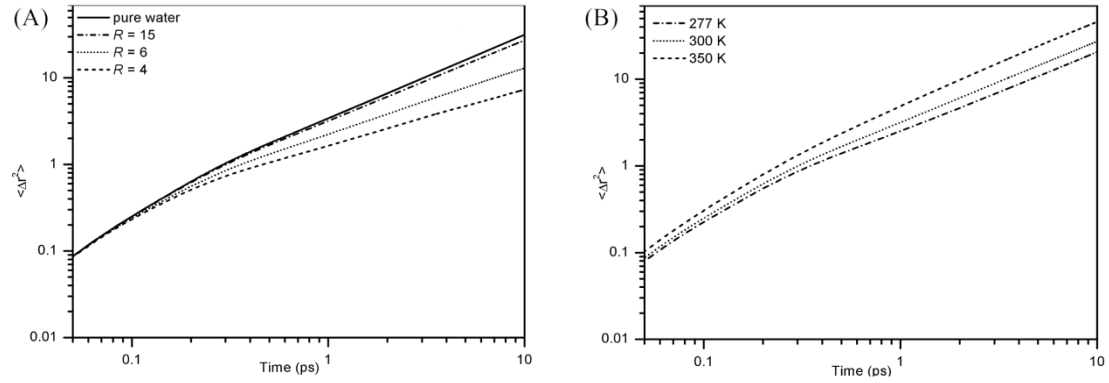

Figure S6: Mean square displacement profile. (A) The log-log plot of the mean square displacement of the water molecules around the G-quadruplex *vs*. time at a temperature of 300 K. Water molecules within the hydration shell thickness $\overline{R}$=4, 6, and 15 Å of the distance from the G-quadruplex surface are considered. Bulk water is shown by the solid line. (B) The log-log plot of the mean square displacement of the water molecules as a function of temperature is plotted *vs*. time. Water molecules within 15 Å from the surface of G-quadruplex are considered.

Supplementary material:

The concentration and ionic contribution free energy corrections were calculated according to the statistical thermodynamic basis for computation of binding affinities (1). The standard free energy of binding of two ligands, A and B, to form a complex, AB, is $\Delta G^{o}_{AB} = -RT\ln(\frac{C^{o}C_{AB}}{C_{A}C_{B}}) = -RT\ln K_{AB}$, where C° is the 1 M standard concentration, C_i is the concentration of species i, R is the gas constant, and T is absolute temperature.

Since the binding ratio, A : B= BMVC : G-quadruplex = 1:1, this gives C_A= C_B=0.0044 M. Thus, the concentration free energy correction, $\Delta G_{conc} = -RT\ln(\frac{C^{o}C_{AB}}{C_{A}C_{B}}) = -3.24$ kcal/mol, where C_A= C_{AB} and T=300 K.

Furthermore, the relationship between the binding constant K of two ligands A and B and ionic concentration [Na^+] is $m = \frac{\partial \log K}{\partial \log[Na^+]}$. The ionic concentration free energy

correction is computed with the equation, $\Delta G_{ion} = -mRT \ln(\frac{[Na^{+}{}_{\exp}]}{[Na^{+}{}_{sim}]}$.

$\Delta G_{ion} = -mRT \ln(\frac{[Na^{+}{}_{\exp}]}{[Na^{+}{}_{sim}]} = -2.89$ kcal/mol, where m=7.00, $[Na^{+}{}_{sim}]$= 0.075 M, and $[Na^{+}{}_{exp}]$= 0.15 M. The absolute ligand binding free energy, ΔG_{bind}, can be computed as the free energy change of the system with the ligand in the bound and unbound state. The ΔG_{bind} is corrected as $\Delta G_{corrected} = \Delta G_{bind} + \Delta G_{ion} - \Delta G_{conc}$.

Table S1. Contribution free energy corrections

	ΔG_{bind}		$\Delta G_{corrected}$	
state	BMVC0	BMVC	BMVC0	BMVC
End-stacked bound state	-13.1 ± 0.7	-16.0 ± 0.4	-12.7 ± 0.7	-15.6 ± 0.4
Groove surface state	-9.1 ± 0.6	-8.2 ± 0.4	-8.7 ± 0.6	-7.8 ± 0.4

Reference

1. Gilson, M.K., Given, J.A., Bush, B.L. and McCammon, J.A. (1997) The statistical-thermodynamic basis for computation of binding affinities: a critical review. *Biophys. J.*, **72**, 1047-1069.

Optimized drug coordinates:

BMVC
TITLE opt HF/6-31g*
REMARK 1 File created by GaussView 5.0.8 Charge

HETATM	1	C	1.824	-3.790	-0.002	C1	-0.024572
HETATM	2	C	3.232	-3.696	-0.002	C12	-0.197910
HETATM	3	C	3.879	-2.489	-0.002	C13	-0.216301
HETATM	4	C	3.098	-1.335	-0.001	C3	0.380733
HETATM	5	C	1.697	-1.386	-0.000	C2	-0.051205
HETATM	6	C	1.067	-2.621	-0.001	C10	-0.179689
HETATM	7	H	3.828	-4.589	-0.004	H12	0.230030
HETATM	8	H	4.952	-2.437	-0.003	H13	0.246201
HETATM	9	H	-0.007	-2.680	-0.001	H10	0.226437
HETATM	10	C	2.396	0.790	0.000	C5	0.380734
HETATM	11	C	2.337	2.183	0.001	C9	-0.216301
HETATM	12	C	1.098	2.768	0.002	C8	-0.197909
HETATM	13	C	-0.089	2.004	0.002	C7	-0.024574
HETATM	14	C	-0.001	0.614	0.001	C6	-0.179687
HETATM	15	C	1.240	-0.002	0.000	C1	-0.051206
HETATM	16	H	3.230	2.780	0.002	H9	0.246201
HETATM	17	H	1.045	3.839	0.003	H8	0.230030
HETATM	18	H	-0.899	0.022	0.002	H6	0.226438
HETATM	19	C	-1.415	2.616	0.002	C23	-0.118311
HETATM	20	C	-1.707	3.925	-0.006	C24	-0.259849
HETATM	21	H	-2.224	1.907	0.010	H23	0.217335
HETATM	22	H	-0.917	4.652	-0.017	H24	0.228753
HETATM	23	C	1.123	-5.071	-0.002	C14	-0.118317
HETATM	24	C	1.668	-6.297	0.007	C15	-0.259845
HETATM	25	H	0.051	-4.983	-0.008	H14	0.217332
HETATM	26	H	2.735	-6.410	0.017	H15	0.228756
HETATM	27	C	-3.045	4.489	-0.005	C25	0.154204
HETATM	28	C	-3.192	5.887	-0.027	C26	-0.309089
HETATM	29	C	-4.239	3.741	0.017	C30	-0.291728
HETATM	30	C	-4.431	6.457	-0.028	C27	0.169696
HETATM	31	H	-2.332	6.527	-0.045	H26	0.274990
HETATM	32	C	-5.444	4.374	0.014	C29	0.163109
HETATM	33	H	-4.235	2.671	0.034	H30	0.262622
HETATM	34	H	-4.564	7.520	-0.044	H27	0.292240
HETATM	35	H	-6.368	3.830	0.030	H29	0.285201

HETATM	36	C	0.929	-7.546	0.006	C16	0.154200
HETATM	37	C	1.643	-8.757	0.027	C21	-0.309127
HETATM	38	C	-0.476	-7.657	-0.015	C17	-0.291679
HETATM	39	C	0.987	-9.953	0.029	C20	0.169736
HETATM	40	H	2.715	-8.759	0.045	H21	0.274986
HETATM	41	C	-1.067	-8.883	-0.011	C18	0.163067
HETATM	42	H	-1.110	-6.794	-0.032	H17	0.262629
HETATM	43	H	1.513	-10.886	0.045	H20	0.292254
HETATM	44	H	-2.133	-8.995	-0.027	H18	0.285204
HETATM	45	C	-6.877	6.351	0.029	C31	-0.326619
HETATM	46	H	-7.557	5.791	-0.593	H311	0.236211
HETATM	47	H	-7.238	6.375	1.048	H312	0.245818
HETATM	48	H	-6.797	7.356	-0.354	H313	0.236747
HETATM	49	C	-1.042	-11.324	-0.026	C22	-0.326645
HETATM	50	H	-1.917	-11.280	0.602	H221	0.236296
HETATM	51	H	-1.324	-11.555	-1.044	H222	0.245776
HETATM	52	H	-0.377	-12.085	0.350	H223	0.236715
HETATM	53	N	3.496	-0.025	-0.001	N4	-0.938768
HETATM	54	H	4.441	0.287	-0.001	H4	0.416505
HETATM	55	N	-5.547	5.714	-0.011	N19	-0.613927
HETATM	56	N	-0.352	-10.020	0.013	N28	-0.613928
END							

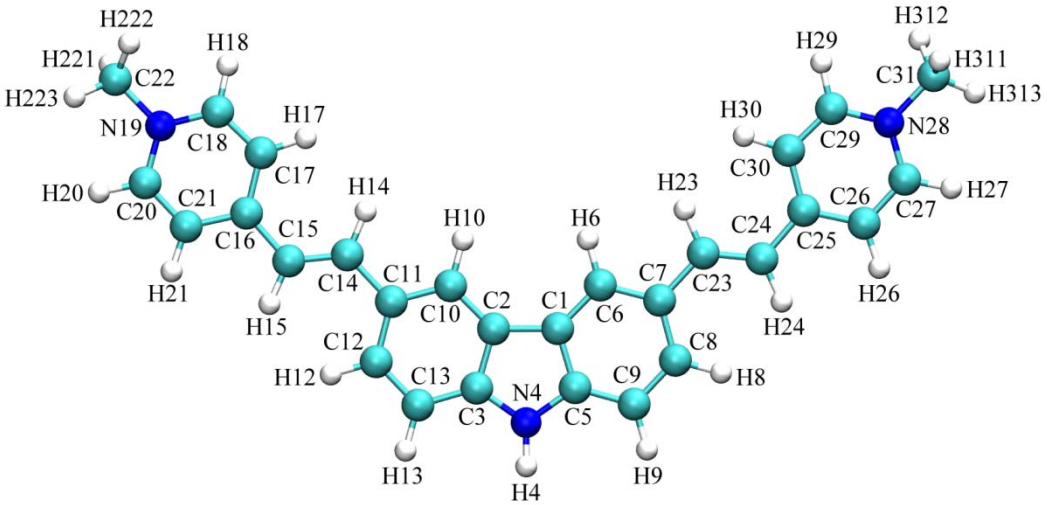

BMVC0

TITLE	opt HF/6-31g*						
REMARK	1 File created by GaussView 5.0.8						Charge
HETATM	1	C	1.860	-3.760	0.203	C1	0.002975
HETATM	2	C	3.264	-3.676	0.244	C12	-0.218122
HETATM	3	C	3.929	-2.473	0.179	C13	-0.228673
HETATM	4	C	3.171	-1.312	0.079	C3	0.364383
HETATM	5	C	1.773	-1.358	0.052	C2	-0.044675
HETATM	6	C	1.126	-2.586	0.119	C10	-0.208212
HETATM	7	H	3.841	-4.576	0.348	H12	0.206715
HETATM	8	H	5.004	-2.437	0.218	H13	0.206277
HETATM	9	H	0.051	-2.630	0.099	H10	0.212651
HETATM	10	C	2.469	0.815	-0.071	C5	0.364381
HETATM	11	C	2.387	2.199	-0.170	C9	-0.228673
HETATM	12	C	1.137	2.770	-0.237	C8	-0.218122
HETATM	13	C	-0.041	2.002	-0.199	C7	0.002975
HETATM	14	C	0.068	0.621	-0.116	C6	-0.208212
HETATM	15	C	1.318	0.020	-0.046	C1	-0.044674
HETATM	16	H	3.272	2.810	-0.208	H9	0.206277
HETATM	17	H	1.065	3.837	-0.341	H8	0.206714
HETATM	18	H	-0.822	0.017	-0.098	H6	0.212650
HETATM	19	C	-1.386	2.610	-0.254	C23	-0.183920
HETATM	20	C	-1.701	3.866	0.041	C24	-0.201248
HETATM	21	H	-2.173	1.932	-0.538	H23	0.189245
HETATM	22	H	-0.931	4.531	0.397	H24	0.187630
HETATM	23	C	1.142	-5.049	0.255	C14	-0.183916
HETATM	24	C	1.637	-6.246	-0.039	C15	-0.201252
HETATM	25	H	0.105	-4.973	0.538	H14	0.189246
HETATM	26	H	2.652	-6.321	-0.392	H15	0.187631
HETATM	27	C	-3.049	4.465	-0.027	C25	0.029110
HETATM	28	C	-3.325	5.608	0.714	C26	-0.222571
HETATM	29	C	-4.077	3.944	-0.815	C30	-0.215143
HETATM	30	C	-4.581	6.196	0.693	C27	-0.227985
HETATM	31	H	-2.553	6.043	1.324	H26	0.199077
HETATM	32	C	-5.326	4.530	-0.833	C29	-0.218730
HETATM	33	H	-3.895	3.085	-1.434	H30	0.203131
HETATM	34	H	-4.759	7.077	1.285	H27	0.195878
HETATM	35	H	-6.097	4.105	-1.454	H29	0.195495
HETATM	36	C	0.910	-7.530	0.027	C16	0.029108

HETATM	37	C	1.370	-8.613	-0.714	C21	-0.222573
HETATM	38	C	-0.228	-7.724	0.813	C17	-0.215143
HETATM	39	C	0.711	-9.832	-0.694	C20	-0.227963
HETATM	40	H	2.251	-8.502	-1.322	H21	0.199078
HETATM	41	C	-0.883	-8.938	0.829	C18	-0.218757
HETATM	42	H	-0.594	-6.925	1.432	H17	0.203132
HETATM	43	H	1.093	-10.646	-1.286	H20	0.195876
HETATM	44	H	-1.756	-9.055	1.448	H18	0.195491
HETATM	45	C	-6.978	6.296	-0.111	C31	-0.507528
HETATM	46	H	-7.253	6.585	-1.121	H311	0.176983
HETATM	47	H	-7.735	5.605	0.247	H312	0.177486
HETATM	48	H	-7.019	7.184	0.511	H313	0.173251
HETATM	49	C	-1.158	-11.340	0.103	C22	-0.507509
HETATM	50	H	-1.227	-11.727	1.115	H221	0.176796
HETATM	51	H	-2.171	-11.238	-0.275	H222	0.177668
HETATM	52	H	-0.651	-12.082	-0.502	H223	0.173245
HETATM	53	N	3.577	0.001	0.005	N4	-0.953462
HETATM	54	H	4.519	0.312	0.006	H4	0.390176
HETATM	55	C	-0.428	-10.017	0.073	C19	0.038167
HETATM	56	C	-5.605	5.667	-0.077	C28	0.038167
END